



ARCHIVIO ISTITUZIONALE DELLA RICERCA

Alma Mater Studiorum Università di Bologna Archivio istituzionale della ricerca

Surface modification of nanocellulose through carbamate link for a selective release of chemotherapeutics

This is the final peer-reviewed author's accepted manuscript (postprint) of the following publication:

Published Version:

Surface modification of nanocellulose through carbamate link for a selective release of chemotherapeutics / Tortorella S.; Maturi M.; Dapporto F.; Spanu C.; Sambri L.; Comes Franchini M.; Chiariello M.; Locatelli E.. - In: CELLULOSE. - ISSN 0969-0239. - ELETTRONICO. - 27:(2020), pp. 8503-8511. [10.1007/s10570-020-03390-5]

This version is available at: <https://hdl.handle.net/11585/788419> since: 2022-02-01

Published:

DOI: <http://doi.org/10.1007/s10570-020-03390-5>

Terms of use:

Some rights reserved. The terms and conditions for the reuse of this version of the manuscript are specified in the publishing policy. For all terms of use and more information see the publisher's website.

(Article begins on next page)

This item was downloaded from IRIS Università di Bologna (<https://cris.unibo.it/>).
When citing, please refer to the published version.

This is the final peer-reviewed accepted manuscript of:

Silvia Tortorella, Mirko Maturi, Francesca Dapporto, Chiara Spanu, Letizia Sambri, Mauro Comes Franchini, Mario Chiariello & Erica Locatelli “Surface modification of nanocellulose through carbamate link for a selective release of chemotherapeutics” *Cellulose*, 2020, 27(15), 8503-8511.

The final published version is available online at: <https://dx.doi.org/10.1007/s10570-020-03390-5>

Terms of use:

Some rights reserved. The terms and conditions for the reuse of this version of the manuscript are specified in the publishing policy. For all terms of use and more information see the publisher's website.

This item was downloaded from IRIS Università di Bologna (<https://cris.unibo.it/>)

When citing, please refer to the published version.

1 **Surface Modification of Nanocellulose through** 2 **Carbamate Link for a Selective Release of** 3 **Chemotherapeutics**

4 Silvia Tortorella,^a Mirko Maturi,^a Francesca Dapporto,^b Chiara Spanu,^a Letizia
5 Sambri,^a Mauro Comes Franchini,^a Mario Chiariello,^b Erica Locatelli^{a*}

6

7 *(a) Department of Industrial Chemistry “Toso Montanari”, Viale Risorgimento 4,*
8 *40136, Bologna, Italy.*

9 *(b) Consiglio Nazionale delle Ricerche (CNR), Istituto di Fisiologia Clinica (IFC),*
10 *via Fioentina 1, 53100, Siena, Italy.*

11

12 Email: erica.locatelli2@unibo.it

13

14

15 **Abstract**

16 Herein we report the synthesis of cellulose nanocrystals covalently bound to a model
17 chemotherapeutic drug (DOXO) via a novel spacer arm, which acts both as linker and as selective
18 releasing agent. The carbamate linkage present in the linker, shows stability in aqueous
19 environments for a wide range of conditions and can only be hydrolyzed in the presence of cells,
20 freeing the active drug, with unmodified chemotherapeutics properties.

21

22 **Keywords**

23 Cellulose nanocrystals, carbamate linker, doxorubicin, selective release.

24

25

26

27 **Introduction**

28 Drug delivery is an important challenge in therapeutics. Setting up new formulations, technologies,
29 and systems for properly achieving the delivery of pharmaceutical compounds is highly required

30 (Locatelli et al. 2014; Grünwald et al. 2016). In the past years, this field of research has increased in
31 terms of studies and publications, mostly focused on polymer-based nanocarriers (Parhi et al. 2012;
32 Sun et al. 2014).

33 Nanomaterials modification for the introduction of active agents onto their surface is the first
34 requisite for creating an effective drug delivery system (Locatelli et al. 2015). Surface modification
35 of nanomaterials with links and spacers has been the key for the introduction of active agents, such
36 as proteins for targeted drug delivery, but it is also a powerful strategy to link on the drug' surface
37 that should be selectively delivered: this is, nowadays, a topic in continuous development (Cellante
38 et al. 2018).

39 Cellulose is the most abundant biopolymer in the world and, in its nanometric form, has wide
40 potential as a component in bio nanocomposites. The use of nanocellulose in drug delivery systems
41 is quite recent: until 2014 nanocellulose was mostly employed for reinforcing the structure of
42 biomaterials (Dufresne 2013; Fatah et al. 2014; Gazzotti et al. 2019; Peres et al. 2019). After 2014,
43 advancements on its chemical processing have strongly pushed the research in biomedical
44 engineering, also due to the low cost of the starting material and the tunable properties of the final
45 nanosystems (Habibi 2014; Khine et al. 2020).

46 One potential and partially explored application of nanocellulose may be in cancer therapy, as
47 nanocarrier for drug transport and release, since its sugar-based backbone allows for easy chemical
48 modification and for a total biocompatibility, absence of cyto- and systemic toxicity, and easy
49 excretion via cell digestion (Lin and Dufresne 2014). Anyways, there are still many issues to be
50 addressed: indeed, the main challenge remains the development of strategies for a controlled surface
51 modification in order to link or incorporate a drug in a stable and reproducible way and, most
52 important, to have a long and controlled release over time.

53 Dash et al. in 2012 worked on cellulose nanocrystals (CNCs) for a new 'alternative' drug delivery
54 system: with the help of aromatic linkers and spacer molecules, they tried the attachment of active
55 amine-containing drugs to the CNCs (Dash and Ragauskas 2012). However, only the introduction
56 of a spacer arm was completed, but neither the creation of a cleavable linker nor the incorporation
57 of the drug was attempted.

58 Carbamates, the esters of carbamic acid, are well known in organic chemistry, especially for their
59 presence in amine-protecting group such as tert-butyloxycarbonyl (Boc), fluorenylmethoxycarbonyl
60 (Fmoc) and carboxybenzyl (Cbz). Due to their hydrolytic stability, carbamates have been used in
61 the design of prodrugs in order to achieve prolonged systemic circulation (Ghosh and Brindisi 2015).
62 Conversion of carbamate prodrugs in body requires the presence of specific enzymes (e.g. esterase)
63 for the release of the parent drug. Upon hydrolysis, carbamate esters release the corresponding
64 alcohol and carbamic acid, which, due to its chemical instability, immediately breaks down to the
65 corresponding amine, thus releasing the free drug and carbon dioxide.

66 Achieving the release of payloads at the target sites in a spatial- and/or time-controlled manner has
67 been reviewed as the real peculiarity of advanced controlled drug delivery systems (DDSs), which
68 can effectively reduce the dosage frequency, while maintaining the drug concentration in targeted
69 organs/tissues for a longer period of time. This became of the utmost importance when applying
70 therapeutics with high toxicological side effects, such as chemotherapeutics. The local, prolonged
71 and smart release of drugs is the only possibility in future for personalized sustained and sustainable
72 therapies, and the research of novel carriers, such the one proposed in this paper, is of tremendous
73 demanding (Liu et al. 2016).

74 Inspired by these medical needs and by the above mentioned data, in this paper we report the linkage
75 of an amino-containing model drug (Doxorubicin, DOXO) onto CNCs via the surface modification
76 of the nanosystem and the creation of a linker that can be easily shortcut by cellular enzymes, finally
77 releasing the active molecules unaltered. Several release conditions were investigated finding an
78 extreme stability of the linkers. Indeed, the release can only happen by an enzyme-cleaved initiation
79 step to separate the linker from the drug and, through decomposition of the linkers, to deliver the
80 unmodified drug (Casey Laizure et al. 2013). With our strategy the drug appears fully active after
81 the release and its efficacy has been proved *in vitro* by cells death assessing.

82

83

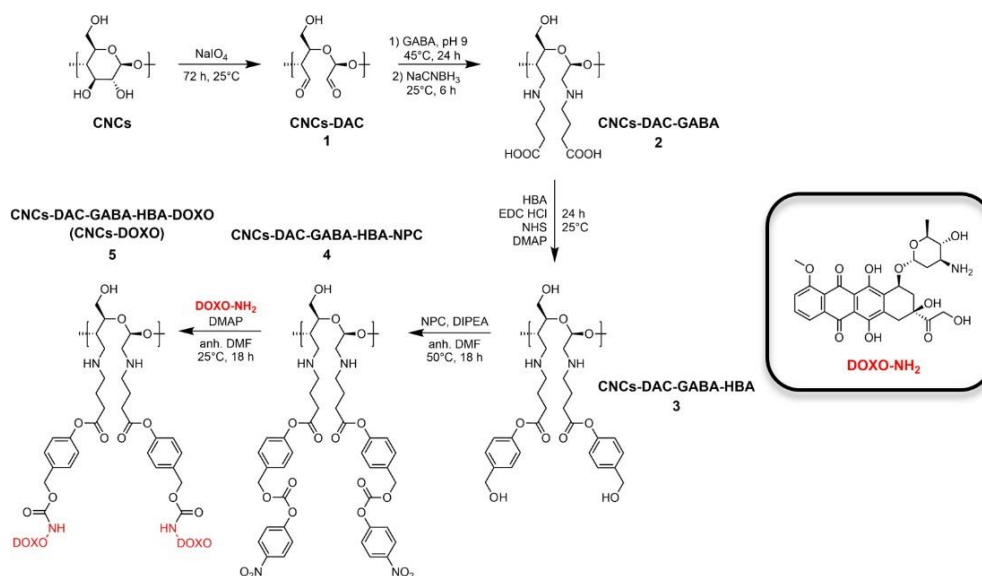
84

85 **Results and Discussion**

86 **Synthesis and Chemical Modification**

87 The nanocarrier was synthesized using pure cellulose filter paper as starting material. This has been
88 digested in acidic environment to produce cellulose nanocrystals, which have been chemically
89 modified on their surface to stably bind the active drug via a series of 5 consecutive reactions (**Fig.**
90 **1**).

91



92

93 **Fig. 1.** Schematic representation of the synthetic step for the preparation of Doxorubicin-loaded
 94 CNCs. Abbreviations: CNCs = cellulose nanocrystals, DAC = cellulose dialdehyde, GABA = γ -
 95 amino butyric acid, HBA = 4-hydroxy benzyl alcohol, EDC HCl = 1-ethyl-3-(3-
 96 dimethylaminopropyl)carbodiimide hydrochloride, NHS = N-hydroxy succinimide, DMAP = 4-
 97 dimethylamino pyridine, NPC = 4-nitrophenyl chloroformate, DIPEA = N,N-diisopropyl-N-
 98 ethylamine, anh. DMF = anhydrous dimethylformamide, DOXO-NH₂ = doxorubicin
 99

100 Cellulose nanocrystals (CNCs) were prepared according to a reported procedure, with slight
 101 modifications (Jiang et al. 2010). The DLS (Dynamic Light Scattering) analysis of hydrolyzed CNCs
 102 revealed a ζ -potential value of -11.0 mV as expected for fully hydroxylated sugars-based structures
 103 (Mahouche-Chergui et al. 2014). The IR spectrum is reported in **Fig. 2a**.

104 The so-obtained CNCs have been then treated with the strong oxidizing agent NaIO₄, so as to lead
 105 to the opening of the sugar ring with selective rupture of the σ C₂-C₃ bond and to the introduction of
 106 two aldehydic residues. The resulting product, dialdehyde cellulose (CNCs-DAC, **1**), showed an
 107 unmodified ζ -potential value of -11.2 mV, in accordance with the introduction of non-charged
 108 functional groups. The IR analysis (**Fig. 2b**) revealed the presence of a signal (even if with poor
 109 intensity) at 1734 cm⁻¹ that can be attributed to the C=O of the aldehydes. The low intensity of the
 110 carbonyl stretching absorption can be related to the equilibrium that exist in water between
 111 aldehydes and geminal diols, catalyzed by both acidic and alkaline conditions, and by the occurrence
 112 of intramolecular hemiacetals (Buschmann et al. 1982). Moreover, the aldehyde content of
 113 periodate-oxidized CNCs was determined to be as high as 0.15 mmol of aldehydes per gram of
 114 CNCs-DAC, revealing extensive oxidation of CNCs surface.

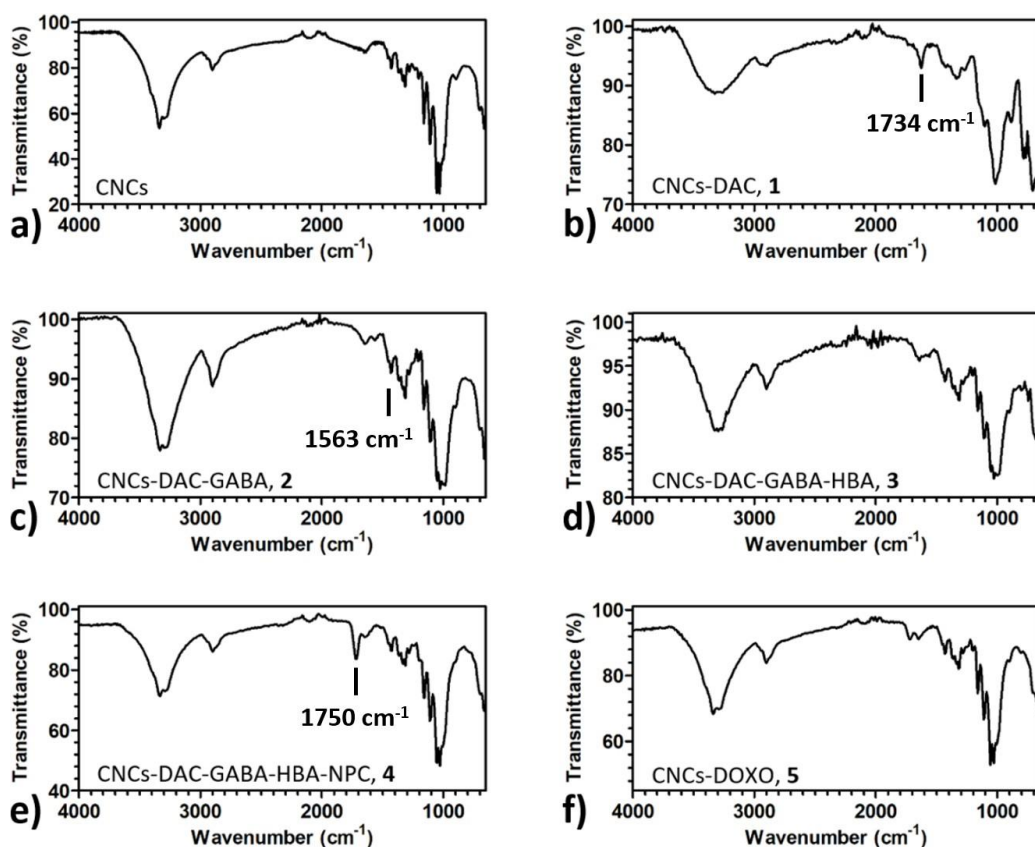
115 CNCs-DAC has been then coupled with γ -aminobutyric acid (GABA) through a reductive amination
 116 in presence of the reducing agent sodium cyanoborohydride (NaCNBH₃): in this reaction, each of
 117 the CNCs aldehyde groups react with the amino group presents in the GABA, thus forming an imine

118 (Schiff base), which is then reduced in the second step, linking the GABA residues to the cellulose
119 backbone through stable amino groups. The obtained product (CNCs-DAC-GABA, **2**) is then
120 purified and characterized: the ζ -potential value has been found equal to - 31.6 mV, which agrees
121 with the introduction of carboxylic groups that are generally deprotonated at neutral pH and able to
122 confer a high negative surface charge. The FTIR analysis (**Fig. 2c**) showed the disappearance of the
123 signal attributed to the aldehyde groups at 1734 cm^{-1} and the appearance of a new signal at 1563 cm^{-1}
124 related to the stretching of N-H bonds.

125 At this point, the nucleophilic substitution with the aromatic linker 4-hydroxybenzyl alcohol (HBA)
126 has been carried out in presence of the coupling agent 1-ethyl-3-(3-dimethylamino propyl)
127 carbodiimide hydrochloride (EDC-HCl) that allows the esterification reaction to proceed in water.
128 The obtained CNCs-DAC-GABA-HBA, **3** presents a ζ -potential value of -15.2 mV, in agreement
129 with the disappearance of -COOH groups in favor of less charged hydroxyl groups. The FTIR
130 analysis (**Fig. 2d**) showed little or no variation in comparison to the previous one.

131 Dash and Ragauskas described the synthesis until this step, but nothing more was attempted for the
132 actual linkage of a drug to CNCs (Dash and Ragauskas 2012). In order to proceed with the
133 functionalization of CNCs and the creation of a cleavable linker, an acylation reaction with 4-
134 nitrophenylchloroformiate was performed in anhydrous DMF. The product (CNCs-DAC-GABA-
135 HBA-NPC, **4**) presents now a carbonate group, suitable for nucleophilic substitution with amino
136 groups. Since this functional group tends to hydrolyze in aqueous environments, the HBA-linked
137 CNCs has been preventively freeze-dried so as to remove most of the water before dissolution in
138 DMF. ζ -potential analysis was not performed because of this inconvenience. Anyways, the FTIR
139 analysis (**Fig. 2e**) showed an intense signal appearing at 1750 cm^{-1} due to the carbonate group, thus
140 confirming the reaction's success.

141 Finally, an amino containing drug could be loaded to CNCs by nucleophilic substitution on the
142 carbonate group on the linker (**Fig. 2f**). As a model drug, Doxorubicin was selected since it contains
143 a single amino group able to react with the linker, and it produces a strong fluorescence that allows
144 for its easy determination and quantification. The selected solvent for the coupling reaction remains
145 anhydrous DMF, but the final product (CNCs-DAC-GABA-HBA-DOXO or CNCs-DOXO, **5**) can
146 be re-dispersed in water after purification, due to the creation of water-stable carbamide bonds. A
147 strong red coloration easily indicates that the reaction proceeds in the desired way and that
148 Doxorubicin has been linked to CNCs. Fluorometric analysis revealed a Doxorubicin loading equal
149 to 0.25% w/w, which is a satisfactory result since only the surface of CNCs can be exploited for
150 functionalization, while the entire core of the nanosystem remains unaffected by the reactions.



151151

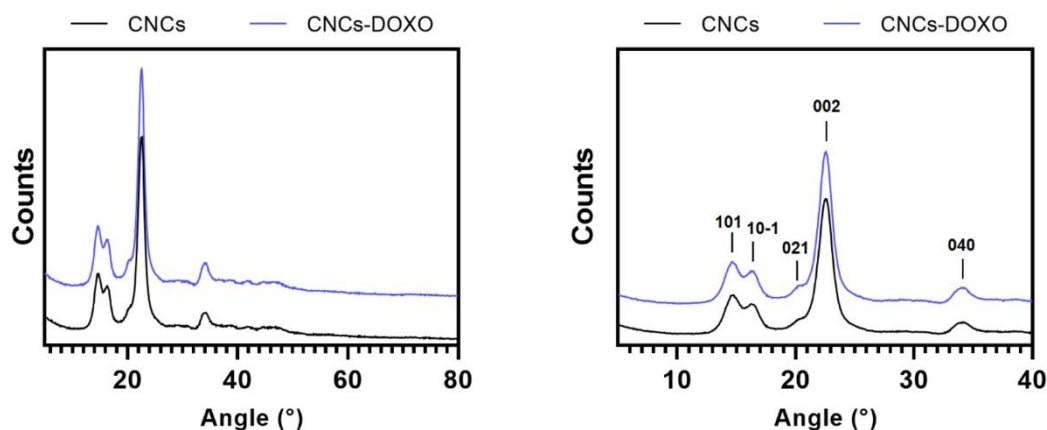
152 **Fig. 2.** ATR-FTIR analysis of the modified cellulose products. CNCs (a); CNCs-DAC, **1** (b); CNCs-
 153 DAC-GABA, **2** (c); CNCs-DAC-GABA, **3** (d); CNCs-DAC-GABA-NPC, **4** (e) and CNCs-DOXO,
 154 **5** (f)

155

156 The mechanism of drug release by this carbamate linker was also discussed by Dash et al., who
 157 theorized the possible drug release via 1-6 elimination of the 4-hydroxy benzyl alcohol. This would
 158 lead to the release of DOXO-NH-CO-O-CH₂PhOH rather than DOXO-NH₂, with unknown effects
 159 on the drug efficacy. In order to demonstrate the efficient release of the pristine drug, we
 160 analyzed by ¹H-NMR the chemical nature of the released species at different pH
 161 (**Supplementary Fig. 2**). At pH 12, DOXO-NH₂ was released without the presence of any sign
 162 of 1-6 elimination of the 4-hydroxy benzyl alcohol, therefore demonstrating the integrity of the
 163 released drug by cleavage of the carbamate bond.

164 The crystallinity of CNCs was confirmed to be unchanged during the conjugation steps by applying
 165 XRD on freeze-dried CNCs-DOXO compared to pristine CNCs (**Fig. 3** and **Supplementary Table**
 166 **2**). This analysis revealed no variation in the crystallinity of CNCs after the formation of the DOXO
 167 linkage.

168168



169169

170 **Fig. 3.** XRD analysis (Cu K α) on freeze-died CNCs compared to CNCs-DOXO. Full spectrum
 171 (left) and its expansion with the *hkl* assignment of the peaks (right).

172172

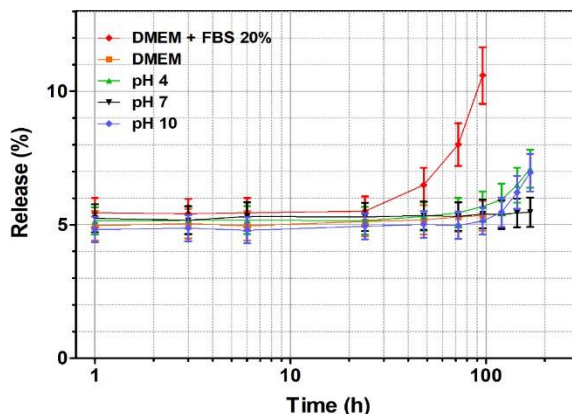
173173

174174

175 Release studies

176 In order to investigate the stability of the carbamate linker and the conditions required to achieve
 177 drug release in vitro, several tests have been performed. In particular, CNCs-DOXO was incubated
 178 at 37°C in D.I. water (pH 6.5), in alkaline (pH 10) and acid (pH 4.5) environments, in DMEM and
 179 finally in DMEM containing 20% of fetal bovine serum (FBS). Drug release was followed over 96
 180 h or 1 week when possible and compared to the total amount of doxorubicin loaded onto CNCs (**Fig.**
 181 **4**). A burst release of drug (around 5.5% of the total) was observed within the first hour
 182 independently on the release medium: this could be related to the release of physisorbed Doxorubicin
 183 from CNCs, not related to the cleavage of any covalent linking. Interestingly, little drug release was
 184 observed only in the presence of FBS after at least 24 h, revealing the great stability of the proposed
 185 linker in aqueous environment. We believe enzymes and/or proteins in FBS are able to partially
 186 trigger the release of DOXO, with an empirical kinetics by which the amount of released drug is
 187 proportional to squared time (**Supplementary Fig. 3 and 4**). As expected, after 96 h DMEM
 188 medium starts to degrade: this is a peculiar property of this agent which helps biologists to monitor
 189 cell growth and maintenance, but does not allow us to prolong the corresponding release study
 190 longer.

191191

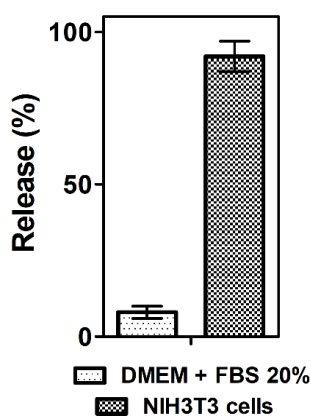


192192

193 **Fig. 4.** Release kinetics of Doxorubicin from CNCs-DOXO in different solutions at 37°C,
 194 determined by fluorometric analysis. Release is observed in DMEM + FBS 20%.

195195

196 Since the drug binding to the nanocarrier demonstrated its stability in normal conditions, we tested
 197 whether the release of DOXO could be triggered by cells themselves, which contain a much greater
 198 variety of enzymes (such as carboxylesterases) that could cleave the carbamate linker. In order to
 199 explore that, CNCs-DOXO has been dispersed in cell culture media containing NIH3T3 cells. After
 200 96 h of incubation at 37°C, a portion of the medium is withdrawn and centrifugated to remove
 201 nanostructures and cells. Fluorescence analysis on the obtained supernatant revealed that around
 202 94% of the CNCs-loaded DOXO was released as free drug, revealing that the complete release of
 203 DOXO can only be achieved by the direct action of cells, while the drug remains stably connected
 204 to cellulose in non-biological systems (**Fig. 5**).



205205

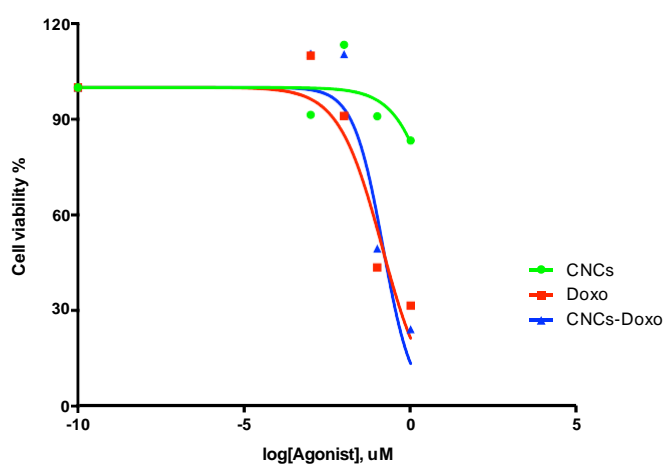
206 **Fig. 5:** Comparison between the released amount of Doxorubicin after 72 h of incubation at 37°C
 207 either in DMEM + FBS 20% or in NIH3T3 cell culture.

208208

209 In vitro studies – Cell Viability Assay

210 The cytotoxicity of CNCs-DOXO was evaluated in NIH3T3 cells by a MTS cell viability assay.
211 Specifically, NIH3T3 cells were treated with increasing concentrations of CNCs-DOXO and
212 compared to equivalent amounts of bare CNCs and free DOXO (**Fig. 6**). Interestingly, the obtained
213 IC_{50} values showed almost identical effects of free doxorubicin ($IC_{50} = 1.139 \mu M$) and CNCs-DOXO
214 ($IC_{50} = 1.148 \mu M$), confirming that cells are able to cut the carbamate linker between CNCs and
215 DOXO, thereby releasing the drug for its cytotoxic action. Importantly, bare CNCs showed very
216 little toxicity at concentrations required for carrying sufficient concentrations of active DOXO (IC_{50}
217 $= 9.505 \mu M$).

218



219

220

221 **Fig. 6.** Cell viability assay in NIH3T3 cells. MTS assay was performed after 72 h treatment of
222 NIH3T3 cells with different concentrations of CNCs, DOXO and CNCs-DOXO, to establish relative
223 IC_{50} values. The results shown are averages of triplicate samples from a typical experiment.

224

225

226 Conclusions

227 In conclusion, we have reported for the first time an effective linker based on carbamate cleavable
228 group for the attachment of model drug (Doxorubicin) to nanocellulose crystal backbone. The
229 protocol for linking the drug is reproducible and easy to handle. The linker, consisting of a spacer
230 arm and the carbamate prodrug, has been proved to be stable under harsh conditions, such as basic
231 or acidic pH. On the other hand, the release of the active and unaltered drug is achieved in almost
232 quantitative way in presence of cells owning proper enzymes for carbamate cleavage.

233 To the best of our knowledge this surface modification of CNCs represents the first successful
234 obtainment of a cleavable linker for incorporation of drugs, thus allowing for the very first time the

235 usage of nanocellulose as proper smart drug delivery system. This modern approach represents the
236 first step towards the use of completely bio-based nanomaterials able to ensure more stimulus-
237 sensitive and sustained nanomedicine for clinical applications.
238238

239 **Experimental section**

240 All chemicals have been purchased from Sigma-Aldrich Co. (St Louis, MO, USA) and used as
241 received. Amount of DOXO linked to the nanocarrier was determined by fluorescence analysis with
242 an Edimburg FLSP920 spectrofluorimeter equipped with a 450 W Xenon arc lamp. All aqueous
243 solutions were prepared with deionized water obtained using an ultrafiltration system (Milli-Q;
244 EMD Millipore, Billerica, MA, USA) with a measured resistivity above 18 M Ω /cm. XRD analysis
245 has been performed with a vertical goniometric diffractometer (Bragg – Brentano geometry) Philips
246 PW 1050/81 with a PW 1710 chain counting employing Cu K α radiation. **¹H-NMR spectra were
247 obtained on a Varian Inova (14.09 T, 600 MHz) NMR spectrometer. In all recorded spectra,
248 chemical shifts have been reported in ppm of frequency relative to the residual solvent signals for
249 both nuclei (¹H: 4.79 ppm for D₂O). Solvent-suppressed ¹H-NMR spectra have been recorded with
250 pre-saturation pulse sequences.**

251251

252 **Synthesis of CNCs**

253 1.5 g of Whatman® cellulose filter paper is finely cut and placed in a 250 mL round-bottomed flask.
254 At this point, 25 mL of ice-cold 4 M aqueous HCl solution are added under stirring. After all the
255 filter paper was soaked in the acid solution, the flask is moved to an oil bath set at 80°C under
256 continuous stirring for 4 h. Hydrolysis is stopped by addition of 70 mL of cold water. Then, the
257 milky suspension is summarily purified by centrifugation (6000 rpm, 15 min) and redispersion in
258 water, and finally by dialysis. Reaction yield (68%) was determined by gravimetric analysis of the
259 final aqueous dispersion, and CNCs was stored in the fridge at a concentration of 2%.

260260

261 **Synthesis of CNCs-DAC, 1:**

262 In a 100 mL flask, 15 mL of the 2% CNCs dispersion are added to 155 mg of NaIO₄. The flask is
263 then wrapped in aluminium foil to protect it from the light, and the reaction is allowed to take place
264 for 72 h by stirring at room temperature. Then, the synthesized CNCs-DAC is separated by
265 centrifugation, dispersed in water and dialyzed. The final concentration of DAC was again 2%. The
266 total aldehyde content was determined exploiting the fluorimetric method reported by Nonsuwan in

267 2009, in which aldehydes are reacted with acetoacetanilide and ammonium acetate exploiting
268 Hantzsch's reaction to quantitatively produce a fluorophore. (Nonsuwan et al. 2019).

269269

270 **Synthesis of CNCs-DAC-GABA, 2:**

271 10 mL of 2% CNCs-DAC are added to 10 mL of 0.2 M sodium acetate solution (pH 9) in a 50 mL
272 round-bottomed flask, and stirred for 15 min. Then, 1.143 g of γ -aminobutyric acid (GABA) are
273 added. Reaction is carried out by stirring at 45°C for 24 h. After cooling, 175 mg of NaCNBH₃ are
274 added, and the mixture is further stirred for 6 h. Reaction mixture is purified by dialysis and
275 centrifugation. Gravimetric analysis on the purified product reveals a 32% yield and a concentration
276 of the final solution equal to 0.63% w/w.

277277

278 **Synthesis of CNCs-DAC-GABA-HBA, 3:**

279 From the previous step, 10 mL of a 0.63% dispersion of 2 are transferred to a 50 mL flask, to which
280 576 mg of EDC HCl, 33 mg of NHS, 384 mg of DMAP and 337 mg of HBA are sequentially added.
281 The mixture is magnetically stirred for 24 h at room temperature, then purified by dialysis and
282 freeze-dried. Final yield was 79%.

283283

284 **Synthesis of CNCs-DAC-GABA-HBA-NPC, 4:**

285 In a dry 50 mL flask and under N₂ atmosphere, 78.2 mg of 3 are dispersed in 20 mL of anhydrous
286 DMF. Then, 715 mg of 4-nitrophenyl chloroformate (NPC) and 50 μ L of DIPEA are added. The
287 mixture is placed in an oil bath set at 50°C and stirred for 18 h, after which the mixture was washed
288 by addition of 5 mL of water and successive centrifugation. Then, in order to remove most of the
289 water, the precipitated pellet is dispersed in anhydrous DMF and centrifugated several times, each
290 time discarding the hydrate DMF supernatant. Finally, the pellet was dispersed in 5 mL of anhydrous
291 DMF to proceed with the conjugation of the drug.

292292

293 **Linkage of Doxorubicin: synthesis of CNCs-DAC-GABA-HBA-DOXO,** 294 **5:**

295 The entire amount of product obtained by the previous step is added to 121 mg of DMAP dissolved
296 in 5 mL of anhydrous DMF, in a round-bottomed flask under N₂ flow. Then, 1 mL of 1 mg mL⁻¹

297 doxorubicin solution is added. Coupling reaction is allowed to happen by stirring at room
298 temperature for 18 h, after which the unbound excess of doxorubicin was eliminated by repeated
299 centrifugation and washes with water, until clear supernatant and red pellet were obtained. The
300 suspension is then freeze-dried and stored at room temperature under vacuum.
301301

302 Quantification of Doxorubicin

303 The amount of doxorubicin (DOXO) in all solutions was determined by fluorometric analysis. Four
304 standard CNCs aqueous solutions at 0.1, 0.2, 0.4 and 0.8 $\mu\text{g mL}^{-1}$ are prepared and their fluorescence
305 emission intensity was detected at 594 nm while exciting at 288 nm. Linear correlation was observed
306 between the counts at the detector and the concentrations, allowing to use fluorescence intensity to
307 measure DOXO concentration, maintaining constant all other experimental parameters
308 (Supplementary Fig. 1).
309309

310 NMR analysis of the released species

311 In order to establish the chemical nature of the released species at different pH, 15 mg of freeze-
312 dried CNCs-DOXO have been dispersed in 1.5 mL of D₂O and divided in three 500 μL portions that
313 are added to 500 μL of 2 M, 0.02 M and 0.0002 M NaOH in H₂O, respectively, to achieve pH values
314 of 10, 12 and 14. At pH 12 the solution turned purple to the deprotonation of DOXO and blue at pH
315 14 due to DOXO decomposition. After overnight incubation at room temperature, samples have
316 been acidified with aqueous HCl and the dispersions have been microfiltered using 440 nm pore-
317 size syringe filters and underwent ¹H-NMR analysis with solvent suppression pulse sequence.
318318

319 Release Studies

320 Release studies were performed by placing 800 μL of a 25 mg mL^{-1} dispersion of CNCs-DOXO
321 inside a Slide-A-Lyzed MINI dialysis device equipped with a membrane with MWCO of 2 kDa and
322 placed into 10 mL of the release medium at 37°C. At predetermined time steps, 2 mL of the release
323 medium are withdrawn to undergo free DOXO quantification by fluorescence analysis and replaced
324 with 2 mL of pure water at 37°C. Buffer at pH 7 was prepared using NaH₂PO₄/Na₂HPO₄ 0.1 M,
325 buffer at pH 4 using CH₃COOH/CH₃COONa 0.1 M and at pH 10 using NaHCO₃/Na₂CO₃ 0.1 M.
326326

327 **In vitro studies – Cell Viability Assay**

328 The antiproliferative effect of CNCs, DOXO and CNCs-DOXO in NIH3T3 cells was measured
329 using the CellTiter 96 AQueous One Solution Cell Proliferation Assay Kit (Promega, Madison, WI,
330 USA), following the manufacturer’s protocol. Briefly, approximately 1×10^3 cells were seeded into
331 each well of a flat-bottom 96-well cell culture plate in 100 μL of recommended culture medium and
332 were allowed to grow for 24 h at 37°C with 5% CO_2 . After 24 h of incubation, culture medium was
333 replaced by fresh medium containing the different test agents. The concentrations of CNCs, DOXO
334 and CNCs-DOXO were gradually increased from 0 to 10 μM (0.000, 0.001, 0.010, 0.100, 1.000,
335 10.000 μM). Seeded 96-well plates were then incubated for 72 h at 37°C with 5% CO_2 . 20 μL of
336 CellTiter 96 AQueous One Solution Cell Proliferation Assay reagent were then added for 2 h at 37
337 °C. The signal was detected using VersaMax MicroPlate Reader (Molecular Device, San Jose, CA
338 USA). The relative growth (compared with the cell viability at 0 h) of the cells was then calculated
339 using the equation: $[A]_T/[A]_{T_0}$, where $[A]_T$ is the absorbance at time point T and $[A]_{T_0}$ is the
340 absorbance at 0 h. The assay was performed in triplicate.

341

342

343 **References**

- 344 Buschmann H-J, Dutkiewicz E, Knoche W (1982) The Reversible Hydration of Carbonyl
345 Compounds in Aqueous Solution Part II: The Kinetics of the Keto/Gem-diol Transition.
346 *Berichte der Bunsengesellschaft für Phys Chemie* 86:129–134.
347 <https://doi.org/10.1002/bbpc.19820860208>
- 348 Casey Laizure S, Herring V, Hu Z, et al (2013) The Role of Human Carboxylesterases in Drug
349 Metabolism: Have We Overlooked Their Importance? *Pharmacother J Hum Pharmacol Drug*
350 *Ther* 33:210–222. <https://doi.org/10.1002/phar.1194>
- 351 Cellante L, Costa R, Monaco I, et al (2018) One-step esterification of nanocellulose in a Brønsted
352 acid ionic liquid for delivery to glioblastoma cancer cells. *New J Chem* 42:5237–5242.
353 <https://doi.org/10.1039/C7NJ04633B>
- 354 Dash R, Ragauskas AJ (2012) Synthesis of a novel cellulose nanowhisker-based drug delivery
355 system. *RSC Adv* 2:3403–3409. <https://doi.org/10.1039/c2ra01071b>
- 356 Dufresne A (2013) Nanocellulose: a new ageless bionanomaterial. *Mater Today* 16:220–227.
357 <https://doi.org/10.1016/j.mattod.2013.06.004>
- 358 Fatah I, Khalil H, Hossain M, et al (2014) Exploration of a Chemo-Mechanical Technique for the
359 Isolation of Nanofibrillated Cellulosic Fiber from Oil Palm Empty Fruit Bunch as a
360 Reinforcing Agent in Composites Materials. *Polymers (Basel)* 6:2611–2624.
361 <https://doi.org/10.3390/polym6102611>

- 362 Gazzotti S, Rampazzo R, Hakkarainen M, et al (2019) Cellulose nanofibrils as reinforcing agents
363 for PLA-based nanocomposites: An in situ approach. *Compos Sci Technol* 171:94–102.
364 <https://doi.org/10.1016/j.compscitech.2018.12.015>
- 365 Ghosh AK, Brindisi M (2015) Organic Carbamates in Drug Design and Medicinal Chemistry. *J*
366 *Med Chem* 58:2895–2940. <https://doi.org/10.1021/jm501371s>
- 367 Grünwald B, Vandooren J, Locatelli E, et al (2016) Matrix metalloproteinase-9 (MMP-9) as an
368 activator of nanosystems for targeted drug delivery in pancreatic cancer. *J Control Release*
369 239:39–48. <https://doi.org/10.1016/j.jconrel.2016.08.016>
- 370 Habibi Y (2014) Key advances in the chemical modification of nanocelluloses. *Chem Soc Rev*
371 43:1519–1542. <https://doi.org/10.1039/C3CS60204D>
- 372 Jiang F, Esker AR, Roman M (2010) Acid-Catalyzed and Solvolytic Desulfation of H₂SO₄ -
373 Hydrolyzed Cellulose Nanocrystals. *Langmuir* 26:17919–17925.
374 <https://doi.org/10.1021/la1028405>
- 375 Khine YY, Batchelor R, Raveendran R, Stenzel MH (2020) Photo-Induced Modification of
376 Nanocellulose: The Design of Self-Fluorescent Drug Carriers. *Macromol Rapid Commun*
377 41:1900499. <https://doi.org/10.1002/marc.201900499>
- 378 Lin N, Dufresne A (2014) Nanocellulose in biomedicine: Current status and future prospect. *Eur*
379 *Polym J* 59:302–325. <https://doi.org/10.1016/j.eurpolymj.2014.07.025>
- 380 Liu D, Yang F, Xiong F, Gu N (2016) The Smart Drug Delivery System and Its Clinical Potential.
381 *Theranostics* 6:1306–1323. <https://doi.org/10.7150/thno.14858>
- 382 Locatelli E, Monaco I, Comes Franchini M (2015) Surface modifications of gold nanorods for
383 applications in nanomedicine. *RSC Adv* 5:21681–21699.
384 <https://doi.org/10.1039/C4RA16473C>
- 385 Locatelli E, Naddaka M, Uboldi C, et al (2014) Targeted delivery of silver nanoparticles and
386 alisertib: in vitro and in vivo synergistic effect against glioblastoma. *Nanomedicine* 9:839–
387 849. <https://doi.org/10.2217/nnm.14.1>
- 388 Mahouche-Chergui S, Grohens Y, Balnois E, et al (2014) Adhesion of Silica Particles on Thin
389 Polymer Films Model of Flax Cell Wall. *Mater Sci Appl* 05:953–965.
390 <https://doi.org/10.4236/msa.2014.513097>
- 391 Nonsuwan P, Matsugami A, Hayashi F, et al (2019) Controlling the degradation of an oxidized
392 dextran-based hydrogel independent of the mechanical properties. *Carbohydr Polym*
393 204:131–141. <https://doi.org/10.1016/j.carbpol.2018.09.081>
- 394 Parhi P, Mohanty C, Sahoo SK (2012) Nanotechnology-based combinational drug delivery: an
395 emerging approach for cancer therapy. *Drug Discov Today* 17:1044–1052.
396 <https://doi.org/10.1016/j.drudis.2012.05.010>
- 397 Peres BU, Vidotti HA, de Carvalho LD, et al (2019) Nanocrystalline cellulose as a reinforcing
398 agent for electrospun polyacrylonitrile (PAN) nanofibers. *J Oral Biosci* 61:37–42.

399 <https://doi.org/10.1016/j.job.2018.09.002>
400 Sun T, Zhang YS, Pang B, et al (2014) Engineered Nanoparticles for Drug Delivery in Cancer
401 Therapy. *Angew Chemie Int Ed* 53:n/a-n/a. <https://doi.org/10.1002/anie.201403036>
402